Author/s:
Williamson, AJ;Sims, NA;Thomas, CDL;Lee, PVS;Stevenson, MA;Whitton, RC

Title:
Biomechanical testing of the calcified metacarpal articular surface and its association with subchondral bone microstructure in Thoroughbred racehorses

Date:
2018-03-01

Citation:
Williamson, A. J., Sims, N. A., Thomas, C. D. L., Lee, P. V. S., Stevenson, M. A. & Whitton, R. C. (2018). Biomechanical testing of the calcified metacarpal articular surface and its association with subchondral bone microstructure in Thoroughbred racehorses. Equine Veterinary Journal, 50 (2), pp.255-260. https://doi.org/10.1111/evj.12748.

DR. AMY WILLIAMSON (Orcid ID : 0000-0003-1789-6061)

DR. CHRIS WHITTON (Orcid ID : 0000-0003-0012-4065)

Article type : General Article

Biomechanical testing of the calcified metacarpal articular surface and its association with subchondral bone microstructure in Thoroughbred racehorses

A. Williamson[1], N. A. Sims[2], C. D. L. Thomas[3], P. V. S. Lee[4], M. Stevenson[1] and R. C. Whitton[1*]

[1]Faculty of Veterinary and Agricultural Sciences, University of Melbourne, Melbourne, Australia;

[2]St Vincent's Institute of Medical Research and Department of Medicine, St. Vincent's Hospital, University of Melbourne, Melbourne, Australia;

[3]Melbourne Dental School, University of Melbourne, Melbourne, Australia;

[4]Department of Mechanical Engineering, Melbourne School of Engineering, University of Melbourne, Melbourne, Australia.

*Corresponding author email: cwhitton@unimelb.ed.au

Keywords: horse; fatigue; osteoarthritis; palmar osteochondral disease; subchondral bone

Summary

Background: Palmar/plantar osteochondral disease (POD) and third metacarpal/-tarsal condylar fractures are considered fatigue injuries of subchondral bone (SCB) and calcified cartilage due to repetitive high loads in racehorses. In combination with adaptive changes in SCB in response to race training, the accumulation of SCB fatigue is likely to result in changes of joint surface mechanical properties.

Objectives: To determine the spatial relationship and correlation of calcified articular surface biomechanical properties with SCB microstructure and training history in the distal palmar metacarpal condyle of Thoroughbred racehorses.

Study design: Cross-sectional study.

Methods: Third metacarpal condyles were examined from 31 Thoroughbred horses with micro-computed tomography (micro-CT). Hyaline cartilage was removed and reference point indentation (RPI) mechanical testing of the calcified articular surface was performed. Training histories were obtained from trainers. The association between indentation distance increase (IDI), an inverse RPI measure of toughness, micro-CT, and training variables were assessed using a mixed-effects generalised linear model.

Results: Untrained horses had higher IDI than horses that had commenced training ($P<0.001$). Death as a result of musculoskeletal bone fatigue injury ($P = 0.044$) and presence of POD ($P = 0.05$) were associated with higher IDI. The micro-CT variables connectivity density and trabecular pattern factor were positively ($P = 0.002$) and negatively ($P<0.001$) correlated with IDI, respectively.

Main limitations: The application of RPI to the calcified articular surface is novel and there is a potential for measurement variability with surface unevenness.

Conclusion: Commencement of race training is associated with altered material properties of the calcified articular surface in horses. Reduced articular surface material properties can also be detected in horses that have fatigue injuries of the distal metacarpus and at other sites in the skeleton. Measures of SCB connectivity and trabecular surface shape may be more important determinants of resistance to failure of the calcified articular surface than traditional measures such as SCB volume and density.

Introduction

Palmar/plantar osteochondral disease (POD) and third metacarpal/-tarsal condylar fractures are considered fatigue injuries of racehorse subchondral bone (SCB) and calcified cartilage due to repetitive high loads [1]. Both injuries are characterised by the coalescence of microcracks initiated at the articular surface of the calcified cartilage [2-4]. During rigorous training, SCB remodelling is inhibited allowing accumulation of fatigued bone [4; 5]. When rested following such training, intense focal SCB resorption occurs, immediately under and including the calcified cartilage layer [6]. Both resorption and sclerosis are implicated in acceleration of SCB damage due to assumed changes in local mechanical properties [6; 7]. There has been limited investigation of the biomechanical roles that both SCB and calcified

cartilage play in injury pathogenesis, despite increasing evidence for SCB involvement in articular disease [8-11].

Reference point indentation (RPI) enables in situ mechanical testing that correlates with traditional whole bone mechanical testing [12; 13]. It is inversely correlated with fracture toughness assessed by three-point bending [13]. The device test probe is housed within a reference probe and performs cyclic indentations at a single location. It induces local separation of mineralised collagen fibrils, and microcrack formation, focal bone compaction and radial damage [12; 14]. The indentation distance increase (IDI) between the first and last indentation cycle has successfully demonstrated deterioration of bone material properties in human patients with osteoporotic and atypical femoral fractures, and has been validated for use in equine cortical bone [12; 15; 16].

The purpose of this study was to determine the spatial relationship and correlation of calcified articular surface biomechanical properties with training history and microstructure in the distal palmar metacarpal condyle of Thoroughbred racehorses. We evaluated RPI and micro-computed tomography (microCT) features from horses in various stages of race training. We hypothesised that the calcified articular surface would exhibit marked regional variations in resistance to failure, which would correlate positively with SCB volume and negatively with SCB porosity and damage.

Materials and methods

Samples

Samples were collected within 24 hours of death from Thoroughbred racehorses that underwent post mortem examination at the University of Melbourne, following death or euthanasia at local racetracks or in the referral hospital. Post mortem reports were collected and training histories obtained from trainers. Data collected included age, sex, limb, current work and training status, weeks in work or days spelling, number of race starts, wins and places, prize money earned, and cause of death. Gross metacarpal condylar lesions were subjectively scored as previously described [17]. Specimens with grossly evident articular surface collapse were excluded.

The palmar epiphysis was removed along a line 55^{o} to the frontal plane through the centre of rotation on both condyles using a bandsaw (Barnes[a]). Samples were wrapped in gauze soaked with normal saline (0.9% sodium chloride[a]) or Compound Sodium Lactate (Hartmann's[b]) and stored in ziplock bags at -20^{o}C.

A total of 31 independent metacarpii were required to detect a difference of 0.50 between the null hypothesis correlation of zero and the alternative hypothesis correlation of 0.50 between microstructural and mechanical measures, with a power of 80% using a two-sided hypothesis test with a significance level of 0.05[18]. The study population was initially defined to include a range of ages and work status, to increase microstructural variation and maximise opportunity to find a correlation between microstructural and biomechanical properties [6; 7]. The required samples were then randomly selected from stored cases available that met these definitions, by use of a random number generator.

A left or right metacarpus was randomly selected from each horse for analysis, as there is no evidence for side predilection of SCB injury [17; 19]. Samples were thawed at room temperature prior to each experimental stage. Medial condyles were trimmed to approximately 20 mm lateromedial × 10 mm dorsopalmar × 10 mm deep slabs using a self-irrigated diamond saw (Isomet[d]). The most axial margin was within the parasagittal groove region (Fig 1).

Microstructural analysis

Imaging and microstructural analysis was performed using micro-CT (SkyScan 1172 high resolution micro-CT[e]). Samples were stabilised inside a humidified tube. Exposure parameters were set at 70 kV, 142 µA, and 10 W, with 10.0 µm pixel size, angular rotation step 0.4°, frame averaging 3, exposure time 1750 ms, and using an aluminum copper filter.

Images were analysed with proprietary microCT software (CTAn[e]). Samples were analysed in thirds; region one was designated as axial, region two mid-condyle and region three abaxial (Fig 1). The depth analysed was 6 mm from the most distal point of the articular surface. Mineral density values were calibrated from the attenuation coefficient by use of two hydroxyapatite calibration phantoms[e] and following the microCT manufacturer's standard protocol. The variables connectivity density (ConnDn) and trabecular pattern factor (TbPf) were originally defined in trabecular bone but have here been applied to SCB that demonstrates both trabecular and cortical microstructure. Connectivity density reflects the extent of multiple connections, preventing separation of a structure into two halves [20]. In high bone volume bone structures such as dense SCB, volume increase or porosity reduction are associated with reducing connections. Trabecular pattern factor measures enclosed cavities and reflects surface concavity; increasing porosity and concavity reduce TbPf [21]. Presence or absence of attrition or mineralised projections was recorded.

Mechanical testing

Mechanical testing was performed using RPI (BioDent™ Hfc RPI instrument[f]) fitted with a BP2 probe (test probe 375 µm diameter, 90° cono-spherical, 2.5 µm radius tip) [12]. Hyaline cartilage was removed from the articular surface with a scalpel blade [11]. Sample hydration

was maintained by periodic moistening with Compound Sodium Lactate (Hartmann's[c]). The sample was stabilised on the commercial RPI stage (Active Life stage with XY positioner[h]) [22]. Each indentation was applied as perpendicular to the articular surface as possible [12; 22]. Test parameters were set at twenty-cycle indentation measurements at 10 N force and 2 Hz, based on testing of human cortical bone [12]. Pre-conditioning was set at five cycles, 2 N force and 4 Hz, modified from Diez-Perez 2010 [12]. Measurements were spaced approximately every 1-2 mm across the articular surface based on published cortical bone protocols [12; 23]. The maximum depth of penetration was 134.84 µm which is less than the mean reported thickness of distal metacarpal condylar calcified cartilage (175 µm) [24].

A custom Matlab[g] code was used to determine the increase in penetration distance (IDI) in µm between the first and last indentation cycle. Eighteen discrete measurements were made per region, and the mean used for correlation with regional microCT results.

Data Analysis

Regression analyses

A linear regression model was used to quantify the influence of training history, gross articular pathology and microstructural properties on IDI. There were 34 candidate explanatory variables (Supplementary Item 1), encompassing individual horse, training, history, gross post mortem pathology, microCT pathology, microstructural and RPI (sample storage time and probe re-use) variable pairs. Variables were screened for collinearity and the least biologically plausible of correlated variables excluded where the Pearson product moment correlation ≥0.8, or if the microCT variable did not account for variation in sample volume.

In univariable screening, hypothesised explanatory variables with unconditional associations with IDI that were significant at P≤0.3 (2-sided) were selected for multivariable modelling. Initially, a fixed-effects linear regression model was developed using a backward stepwise variable selection process. All of the explanatory variables that were associated with IDI with P≤0.3 were entered into the model. Explanatory variables were then removed from the model one at a time, beginning with the least significant, until only variables associated with the outcome at P≤0.05 were retained. Each variable that was removed was then added back into the model one by one and retained as a confounder if it was significantly associated with IDI and if it changed the coefficient of any of the other retained explanatory variables in the model by >20%. We assessed biologically plausible two-way interactions between the main effects remaining in the final multivariable model, and none were found to be significant.

To account for lack of independence in the data arising from repeated condylar observations on the same horse the fixed-effects linear regression model was extended to include a zero mean, Gaussian horse-level random effect term. Frequency histograms of the residuals from

the multilevel model and plots of the residuals versus predicted values were constructed to check that the assumptions of normality and homogeneity of variance had been met.

Descriptive analysis was performed using SPSS version 22 (IBM Corp, 2013, IBM SPSS Statistics for Windows: Version 22.0[h]). The fixed- and mixed-effects linear regression modelling was carried out using Stata version 13 (StataCorp, 2013, Stata Statistical Software: Release 13[i]).

Results

Cases

The 31 condyles were randomly selected from 58 available at the start of the study. Descriptive case information is provided in Supplementary Items 1, 2 and 3.

Description of microstructure

Subjectively, extension of dense bone from the SCB plate causing loss of trabecular structure was greatest in the mid-condylar and axial regions (Fig 2a). The extent of dense SCB with loss of trabecular architecture appeared to increase with increasing age. Untrained horses had no to mild loss of SCB trabecular structure. Focal pores were concentrated within the superficial SCB to a depth of 100 µm, and often extended through the calcified cartilage layer into the hyaline cartilage; pores were finely continuous with underlying trabecular bone (Fig 2b). These were common in untrained horses (5/6). Longer more linear voids 100-200 µm in width, extending through dense trabecular bone, were typically located in the mid condylar region; in one horse they were closer to the axial parasagittal region. In 6/16 condyles these channels were surrounded by a ring of hypomineralised bone (Fig 2c), and channels were finely continuous with the articular surface at the scan resolution.

Microfractures of the calcified cartilage, determined as microcracks at 45^{o} to and contiguous with the articular surface, were observed in samples from all ages [4]. Microfractures extended varying lengths in the underlying trabecular bone plate and were contiguous with a resorption space or channel. In 3/6 untrained horses, microfractures were short or fine. Hypermineralised and likely healed microfractures were more common in horses in training older than three years (Supplementary Item 4); small numbers of these microfractures were also present in half of the untrained horses.

Hypermineralised projections extending from calcified cartilage into hyaline cartilage were present in three horses in training. Two horses aged six and seven years additionally had midcondylar resorption channels and articular surface collapse as observed on microCT (Supplementary Item 5). One four-year-old horse had a mineralised projection without articular surface collapse. This horse uniquely had four unassociated voids or pits present on the calcified articular surface (Supplementary Item 6). These voids were located on the axial

margin of the mid condyle, which had underlying resorption channels through a region of dense SCB.

Accumulation of linear voids in the superficial SCB was observed in two cases (2/6), with multiple SCB plate pores present in one case.

Mechanical properties

Surface mechanical properties were uniform across the condyle with no difference in IDI between regions (Supplementary Item 7).

Modelling

Univariable analysis

Following exclusion of highly correlated variables, univariate screening identified 18 of the 27 candidate explanatory variables that were associated with IDI with P≤0.3 (Supplementary item 2). Of these, nine variables were significant at P≤0.05 (Supplementary Item 2). Two non-significant variables, cause of death (P = 0.6) and POD (P = 0.5), were retained due to the biological plausibility of their association with IDI, providing 20 candidate explanatory variables for linear regression modelling.

Multivariable analysis

The fixed effects linear regression model identified 11 explanatory variables that were significantly associated with IDI at the alpha level of 0.05: group (trained or untrained), age, race status, cause of death, gross cartilage wear lines, gross cartilage loss, gross linear fissures, attrition, TbPf, ConnDn and sample storage time. After accounting for unmeasured individual horse-level effects using the mixed-effects linear regression model, five explanatory variables were retained.

Untrained horses had higher IDI than horses that had entered race training (P<0.001, 95% CI 3.92-8.39) (Figure 3). Death as a result of any musculoskeletal fatigue injury and presence of POD were associated with higher IDI compared to other causes, (P = 0.044, 95% CI 0.048-3.62 and P = 0.05, 95% CI 0.038-4.01 respectively). The micro-CT variables connectivity density and trabecular pattern factor were positively (P<0.001, 95% CI 0.49-1.63) and negatively (P = 0.002, 95% CI -0.31- -0.068) correlated respectively with IDI, respectively. Examination of the standardised residuals from the final mixed-effects model identified no significant outliers or lack of normality.

Discussion

In contrast to our hypothesis, we did not find variation in toughness across the calcified articular surface of the third metacarpal medial condyle. However we observed an association

between the initiation of race training and reduced IDI. Two measures of trabecular connectivity were associated with IDI whereas other subchondral bone microstructural measures were not. In addition a higher calcified articular surface IDI was observed in both horses that suffered a catastrophic musculoskeletal injury and horses with POD lesions independently.

The RPI method predominantly assessed the local biomechanical properties of the calcified cartilage, as our maximum probe penetration depth was less than the mean reported thickness of metacarpal condylar calcified cartilage [24]. In particular it is a measure of the propensity for microcrack formation and the calcified cartilage is the site at which microcracks most commonly originate [4; 25]. Therefore changes in the underlying SCB microstructure are unlikely to directly affect surface IDI measurements. However, we expected to observe indirect associations as SCB microstructure is responsive to its loading environment and deterioration of calcified cartilage mechanical properties are a result of that same loading environment.

Regional variation in microstructural and gross biomechanical properties between dorsal-palmar and medial-lateral condyle, and sagittal ridge SCB samples has been described [5; 11; 26; 27]. We observed relatively uniform calcified cartilage biomechanical properties across the metacarpal condyle. This may be a result of the very different homeostatic mechanisms of cartilage and bone; for example bone's ability to actively remodel.

Despite previous correlation with elastic modulus and yield stress in compression testing of diseased equine SCB, bone volume fraction and bone mineral densities were not retained in our model [11]. While bone mineral density has traditionally been used to asses fracture risk, changes in bone toughness and fracture risk have been demonstrated in humans, dogs and rats without commensurate changes in bone mineral density [28-30].

The effect of race training commencement on articular surface IDI may be intensity dependent. Our findings oppose previous nanoindentation testing of equine SCB demonstrating no effect of early preconditioning exercise or early training on elastic modulus [8; 9]. Training has been associated with increased estimated bulk modulus of cortical bone and exercise is associated with reduced cortical bone IDI in mice [31; 32]. Because observations for this study were made at a single point in time it is difficult to determine when calcified articular surface toughness is maximised by race training but a higher risk of fractures that commonly propagate from the calcified cartilage surface is observed in horses in their first year of racing [33].

We identified an increase in IDI of the metacarpal articular surface in horses that have evidence of accumulating bone fatigue both locally in the distal metacarpus (POD) and more

widely in the skeleton (horses that died as a result of any musculoskeletal stress injury). Our findings suggest accumulation of microdamage was not confined to the site of fracture in these cases. This is consistent with the observation of increased bone volume fraction of the distal third metacarpal both in horses with fracture of the third metacarpal condyle or another skeletal site, compared to horses without fracture [6]. The ability of RPI to correlate with global fracture risk has been previously demonstrated, through differentiation of more fragile osteoporotic bone in vivo, and diabetic and bisphosphonate treated cortical bone in vitro [12; 13]. No association of musculoskeletal stress injury has previously been identified with Young's Modulus in equine SCB fatigue testing [34]. Fatigue injury may accumulate preferentially at the calcified articular surface and RPI may be more sensitive to changes associated with microdamage.

Indentation distance increase did increase in the mid-condylar region with the presence of gross POD, consistent with a reduction in SCB plate yield stress identified with severely diseased bone [11]. We observed no significant association between gross linear fissuring of the axial parasagittal groove region and IDI. Changes in parasagittal groove toughness may predispose to metacarpal condylar fracture, although there is no reported association between linear fissures and fracture [8]. Altered calcified cartilage and SCB stiffness has been documented in untrained horses with thickened parasagittal groove calcified cartilage [8]. We also identified three horses in training with mineralised projections extending from the calcified surface into the hyaline cartilage. These projections have previously been found to be stiffer than other mineralised matrix [35]. Although not specifically tested in our study, their presence was not associated with alterations in articular surface IDI, however numbers were small.

Two microstructural variables of SCB were associated with calcified articular surface IDI. Connectivity density, reflecting the extent of multiple connections, was positively correlated with IDI and therefore negatively correlated with toughness [20]. Unlike in osteoporotic bone where increasing connectivity is associated with decreasing bone porosity, in the very dense bone of the distal metacarpus increasing connectivity density values are associated with greater porosity as there are more individual connections. Our findings contrast with previous gross mechanical testing where connectivity was positively correlated with bulk energy to failure (toughness) of SCB plate explants, although connectivity calculations were based on microCT at a lower resolution (45 µm)[11]. Trabecular pattern factor, a measure of concavity of bone surfaces that tends to decrease as porosity increases, was negatively correlated with IDI [21]. Our findings demonstrate an effect of TbPf on articular surface material properties independent of that of ConnDn. Therefore reduced articular surface toughness was associated with greater numbers of pores - producing more individual connections with concave surfaces. This may reflect increased vascularisation of dense bone or focal remodelling activity, a likely result of injury.

There were a number of study limitations. Reference point indentation has not previously been applied to calcified cartilage, and our method may not have resulted in complete hyaline cartilage removal. Reference point indentation was developed to minimise overlying soft tissue effects on bone properties, although incomplete removal may result in increased coefficient of variation [23]. This was addressed by utilising preconditioning to displace soft tissue, and utilising a large number of measures per region of interest [23; 36]. Additionally the articular surface of the condyle is curved and uneven. Every effort was made to maintain the reference probe perpendicular to the visible articular surface, well within the effective probe range of ± 7.5° [22]. In samples with POD lesions the location of the lesions varied in a proximal/distal plane so that the whole lesion was not always within the sample. Sample size calculations were based on detecting a correlation of RPI with microstructural variables, not with historical or post mortem variables. As this was the novel application of RPI to the calcified articular surface, we evaluated all microCT variables as possible explanatory variables in our model. This increases the risk of Type I error.

In conclusion, the large change in SCB microarchitecture and resistance of the calcified surface to injury that occurs when horses commence training coincides with a period when fracture risk at this site is higher. The distal palmar metacarpal articular surface appears to be a site sensitive to fatigue as a reduction in surface material properties can be detected in horses that have developed fatigue injuries at this site and at other sites in the skeleton. Further investigation of bone microstructural properties is warranted based on our bone connectivity and surface shape findings.

Authors' declarations of interests

The authors have no competing interests.

Ethical animal research

The use of animal tissues met the requirements of the University of Melbourne Animal Ethics Committee. Trainers and/or owners gave consent for inclusion of their horses.

Source of funding

This study was funded by Racing Victoria Limited and a University of Melbourne Veterinary Hospital research grant.

Acknowledgements

The authors would like to thank Garry Anderson for statistical advice, Sandra Martig for assistance with sample collection, and Christina Vhranas for assistance with RPI.

Authorship

A. Williamson and R.C. Whitton contributed to study design, data analysis, and preparation of the manuscript; A. Williamson contributed to data collection and study execution; N. Simms and P.V.S. Lee contributed to study design; M. Stevenson contributed to data analysis. All authors contributed to data interpretation and reviewed and approved the final version of the manuscript.

Manufacturers' addresses

[a]HT Barnes, BMSS Butchers Machinery, North Coburg, Victoria, Australia.

[b]Baxter, Old Toongabbie, New South Wales, Australia.

[c]Fresenius Kabi, Friedberg, Germany.

[d]Buehler Ltd, Lake Bluff, Illinois, USA.

[e]Bruker microCT, Kontich, Belgium.

[f]Active Life Scientific, Inc., Santa Barbara, California, USA.

[g]Mathworks, Natick, Massachusetts, USA.

[h]IBM Corp., Armonk, New York, USA.

[i]StataCorp LP, College Station, Texas, USA.

Figure legends

Fig 1: Palmar condyles were removed at 55° to the frontal plane through the centre of rotation. Medial condyles only were selected, and divided into three regions for microstructural and mechanical analysis.

Fig 2: MicroCT images (10.0 µm resolution) of the distal third metacarpal palmar medial condyle from Thoroughbred racehorses (abaxial to the left, axial to the right). a) An untrained horse with multiple pores in the superficial subchondral bone (arrows). b) A two-year-old horse in training with linear channels (arrows), surrounded by hypomineralisation, through dense trabecular subchondral bone in the mid-condylar region. c) A three-year-old horse with densification of subchondral bone and loss of trabecular structure.

Fig 3: Regional box-and-whisker plot of indentation distance increase (IDI) against training status for the distal third metacarpal palmar medial condyle of Thoroughbred racehorses. Group 1: untrained, n = 6; group 2: trained, n = 25. Region 1 = axial, region 2 = mid-condyle, region 3 = abaxial. Group 1>2 (P<0.00005).

Table 1: Estimated regression coefficients and their standard errors from a mixed-effects generalised linear model of factors associated with indentation distance at the calcified articular surface of the distal third metacarpal palmar medial condyle of Thoroughbred racehorses.

Variable	**Categories**	**Coefficient (Standard Error)**	***z***	**P>|z|**	**95% Confidence Interval**
Intercept		12.19 (1.53)	7.96	<0.001	9.19 - 15.19
Group	Untrained	5.83 (1.18)	4.96	<0.001	3.53 - 8.14
	Trained	Reference			
Cause of death	Musculoskeletal fatigue injury	2.23(0.93)	2.40	0.02	0.41 - 4.05[a]
	Other	Reference			
Trabecular pattern factor		-0.20 (0.062)	-3.20	0.001	-0.32 - -0.078
Connectivity density		1.02 (0.30)	3.47	0.001	0.44 - 1.60
Random effect [b]	Variance	SE			

Horse	1.96	0.37

[a]Compared with horses where the cause of death was for other reasons and after adjusting for the effect of training status, trabecular pattern factor, connectivity density and unmeasured, individual horse-level effects, indentation distance at the calcified articular surface of the distal third metacarpal palmar medial condyle for horses where the cause of death was due to musculoskeletal fatigue injury was increased by 2.23 (95% CI 0.41 to 4.05) μm.

[b]Variance and standard error of the variance of the individual horse-level random effect term.

References

[1] Martig, S., Chen, W., Lee, P.V. and Whitton, R.C. (2014) Bone fatigue and its implications for injuries in racehorses. *Equine Vet. J.* **46**, 408-415.

[2] Muir, P., Peterson, A.L., Sample, S.J., Scollay, M.C., Markel, M.D. and Kalscheur, V.L. (2008) Exercise-induced metacarpophalangeal joint adaptation in the Thoroughbred racehorse. *J. Anat.* **213**, 706-717.

[3] Stepnik, M.W., Radtke, C.L., Scollay, M.C., Oshel, P.E., Albrecht, R.M., Santschi, E.M., Markel, M.D. and Muir, P. (2004) Scanning electron microscopic examination of third metacarpal/third metatarsal bone failure surfaces in thoroughbred racehorses with condylar fracture. *Vet. Surg.* **33**, 2-10.

[4] Whitton, R.C., Mirams, M., Mackie, E.J., Anderson, G.A. and Seeman, E. (2013) Exercise-induced inhibition of remodelling is focally offset with fatigue fracture in racehorses. *Osteoporos. Int.* **24**, 2043-2048.

[5] Holmes, J.M., Mirams, M., Mackie, E.J. and Whitton, R.C. (2014) Thoroughbred horses in race training have lower levels of subchondral bone remodelling in highly loaded regions of the distal metacarpus compared to horses resting from training. *Vet. J.* **202**, 443-447.

[6] Whitton, R.C., Trope, G.D., Ghasem-Zadeh, A., Anderson, G.A., Parkin, T.D.H., Mackie, E.J. and Seeman, E. (2010) Third metacarpal condylar fatigue fracture in equine athletes occur within previously modelled subchondral bone. *Bone* **47**, 826-831.

[7] Riggs, C.M. (2002) Fractures--a preventable hazard of racing thoroughbreds? *Vet. J.* **163**, 19-29.

[8] Doube, M., Firth, E.C., Boyde, A. and Bushby, A.J. (2010) Combined nanoindentation testing and scanning electron microscopy of bone and articular calcified cartilage in an equine fracture predilection site. *European Cells and Materials* **19**, 242-251.

[9] Ferguson, V.L., Bushby, A.J., Firth, E.C., Howell, P.G.T. and Boyde, A. (2008) Exercise does not affect stiffness and mineralisation of third metacarpal condylar subarticular calcified tissues in 2 year old thoroughbred racehorses. *European Cells and Materials* **16**, 40-46.

[10] Sniekers, Y.H., Intema, F., Lafeber, F.P., van Osch, G.J., van Leeuwen, J.P., Weinans, H. and Mastbergen, S.C. (2008) A role for subchondral bone changes in the process of osteoarthritis; a micro-CT study of two canine models. *BMC Musculoskeletal Disorders* **9**, 20.

[11] Rubio-Martinez, L.M., Cruz, A.M., Gordon, K. and Hurtig, M.B. (2008) Mechanical properties of subchondral bone in the distal aspect of third metacarpal bones from Thoroughbred racehorses. *Am. J. Vet. Res.* **69**, 1423-1433.

[12] Diez-Perez, A., Guerri, R., Nogues, X., Caceres, E., Pena, M.J., Mellibovsky, L., Randall, C., Bridges, D., Weaver, J.C., Proctor, A., Brimer, D., Koester, K.J., Ritchie, R.O. and Hansma, P.K. (2010) Microindentation for in vivo measurement of bone tissue mechanical properties in humans. *J. Bone Miner. Res.* **25**, 1877-1885.

493 [13] Gallant, M.A., Brown, D.M., Organ, J.M., Allen, M.R. and Burr, D.B. (2013) Reference-
494 point indentation correlates with bone toughness assessed using whole-bone
495 traditional mechanical testing. *Bone* **53**, 301-305.

496

497 [14] Beutel, B.G. and Kennedy, O.D. (2015) Characterization of damage mechanisms
498 associated with reference point indentation in human bone. *Bone* **75**, 1-7.

499

500 [15] Guerri-Fernandez, R.C., Nogues, X., Quesada Gomez, J.M., Torres Del Pliego, E., Puig,
501 L., Garcia-Giralt, N., Yoskovitz, G., Mellibovsky, L., Hansma, P.K. and Diez-Perez, A.
502 (2013) Microindentation for in vivo measurement of bone tissue material properties
503 in atypical femoral fracture patients and controls. *J. Bone Miner. Res.* **28**, 162-168.

504

505 [16] Brimer, D., Herthel, D., Dickinson, M. and Daniel, A. (2010) In-vivo and post mortem
506 investigation of reference point indentation (RPI) in the horse. *J. Bone Miner. Res.*
507 **25**, S372 abstract.

508

509 [17] Barr, E.D., Pinchbeck, G.L., Clegg, P.D., Boyde, A. and Riggs, C.M. (2009) Post mortem
510 evaluation of palmar osteochondral disease (traumatic osteochondrosis) of the
511 metacarpo/metatarsophalangeal joint in Thoroughbred racehorses. *Equine Vet. J.*
512 **41**, 366-371.

513

514 [18] Cohen, J. (1992) A Power Primer. *Psychological Bulletin* **112**, 155-159.

515

516 [19] Riggs, C.M., Whitehouse, G.H. and Boyde, A. (1999) Pathology of the distal condyles
517 of the third metacarpal and third metatarsal bones of the horse. *Equine Vet. J.* **31**,
518 140-148.

519

520 [20] Odgaard, A. and Gundersen, H.J. (1993) Quantification of connectivity in cancellous
521 bone, with special emphasis on 3-D reconstructions. *Bone* **14**, 173-182.

522

[21] Hahn, M., Vogel, M., Pompesius-Kempa, M. and Delling, G. (1992) Trabecular bone pattern factor--a new parameter for simple quantification of bone microarchitecture. *Bone* **13**, 327-330.

[22] Active Life Scientific, I. (2014) Sample positioning, stability and probe sample contact guidance v2.0.

[23] Jenkins, T., Coutts, L.V., Dunlop, D.G., Oreffo, R.O., Cooper, C., Harvey, N.C., Thurner, P.J. and Group, O.S. (2015) Variability in reference point microindentation and recommendations for testing cortical bone: maximum load, sample orientation, mode of use, sample preparation and measurement spacing. *J. Mech. Behav. Biomed. Mater.* **42**, 311-324.

[24] Martinelli, M.J., Eurell, J., Les, C.M., Fyhrie, D. and Bennett, D. (2002) Age-related morphometry of equine calcified cartilage. *Equine Vet. J.* **34**, 274-278.

[25] Turley, S.M., Thambyah, A., Riggs, C.M., Firth, E.C. and Broom, N.D. (2014) Microstructural changes in cartilage and bone related to repetitive overloading in an equine athlete model. *J. Anat.* **224**, 647-658.

[26] Rubio-Martinez, L.M., Cruz, A.M., Gordon, K. and Hurtig, M.B. (2008) Structural characterization of subchondral bone in the distal aspect of third metacarpal bones from Thoroughbred racehorses via micro--computed tomography. *Am. J. Vet. Res.* **69**, 1413-1422.

[27] Riggs, C.M., Whitehouse, G.H. and Boyde, A. (1999) Structural variation of the distal condyles of the third metacarpal and third metatarsal bones in the horse. *Equine Vet. J.* **31**, 130-139.

[28] Aref, M., Gallant, M.A., Organ, J.M., Wallace, J.M., Newman, C.L., Burr, D.B., Brown, D.M. and Allen, M.R. (2013) In vivo reference point indentation reveals positive

effects of raloxifene on mechanical properties following 6 months of treatment in skeletally mature beagle dogs. *Bone* **56**, 449-453.

[29] Sarkar, S., Mitlak, B.H., Wong, M.M., Stock, J.L., Black, D.M. and Harper, K.D. (2002) Relationships between bone mineral density and incident vertebral fracture risk with raloxifene therapy. *J. Bone Miner. Res.* **17**, 1-10.

[30] Hammond, M.A., Gallant, M.A., Burr, D.B. and Wallace, J.M. (2014) Nanoscale changes in collagen are reflected in physical and mechanical properties of bone at the microscale in diabetic rats. *Bone* **60**, 26-32.

[31] Randall, C., Mathews, P., Yurtsev, E., Sahar, N., Kohn, D. and Hansma, P. (2009) The bone diagnostic instrument III: testing mouse femora. *Rev. Sci. Instrum.* **80**, 065108.

[32] McCarthy, R.N. and Jeffcott, L.B. (1992) Effects of treadmill exercise on cortical bone in the third metacarpus of young horses. *Res. Vet. Sci.* **52**, 28-37.

[33] Parkin, T.D., Clegg, P.D., French, N.P., Proudman, C.J., Riggs, C.M., Singer, E.R., Webbon, P.M. and Morgan, K.L. (2004) Horse-level risk factors for fatal distal limb fracture in racing Thoroughbreds in the UK. *Equine Vet. J.* **36**, 513-519.

[34] Martig, S., Lee, P.V., Anderson, G.A. and Whitton, R.C. (2013) Compressive fatigue life of subchondral bone of the metacarpal condyle in thoroughbred racehorses. *Bone* **57**, 392-398.

[35] Boyde, A., Riggs, C.M., Bushby, A.J., McDermott, B., Pinchbeck, G.L. and Clegg, P.D. (2011) Cartilage damage involving extrusion of mineralisable matrix from the articular calcified cartilage and subchondral bone. *European cells & materials* **21**, 470-478.

[36] Setters, A. and Jasiuk, I. (2014) Towards a standardized reference point indentation testing procedure. *J. Mech. Behav. Biomed. Mater.* **34**, 57-65.

Supplementary Information

Supplementary Item 1: Potential explanatory variables for indentation distance increase.

Supplementary Item 2: Univariate screening of variables associated with indentation distance increase.

Supplementary Item 3: Cause of death and gross distal third metacarpal post mortem pathology.

Supplementary Item 4: MicroCT image of the distal third metacarpal palmar medial condyle with hypermineralised microcracks, loss of trabecular bone structure, dense bone and an area of attrition.

Supplementary Item 5: MicroCT image of the distal third metacarpal palmar medial condyle with hypermineralised articular surface projections and an area of marked articular surface collapse.

Supplementary Item 6: MicroCT image of the distal third metacarpal palmar medial condyle with voids or pits present on the calcified articular surface and an unassociated mineralised projection into the hyaline cartilage.

Supplementary Item 7: Regional indentation distance increase (um) and cause of death.

Table 1: Estimated regression coefficients and their standard errors from a mixed-effects generalised linear model of factors associated with indentation distance at the calcified articular surface of the distal third metacarpal palmar medial condyle of Thoroughbred racehorses.

Variable	**Categories**	**Coefficient (Standard Error)**	***z***	**P>|z|**	**95% Confidence Interval**
Intercept		12.19 (1.53)	7.96	<0.0005	9.19 - 15.19
Group	Untrained	5.83 (1.18)	4.96	<0.0005	3.53 - 8.14
	Trained	Reference			
Cause of death	Musculoskeletal fatigue injury	2.23(0.93)	2.40	0.016	0.41 - 4.05[a]
	Other	Reference			
Trabecular pattern factor		-0.20 (0.062)	-3.20	0.001	-0.32 - -0.078
Connectivity density		1.02 (0.30)	3.47	0.001	0.44 - 1.60
Random effect [b]	Variance	SE			
Horse	1.96	0.37			

[a] Compared with horses where the cause of death was for other reasons and after adjusting for the effect of training status, trabecular pattern factor, connectivity density and unmeasured, individual horse-level effects, indentation distance at the calcified articular surface of the distal third metacarpal palmar medial condyle for horses where the cause of death was due to musculoskeletal fatigue injury was increased by 2.23 (95% CI 0.41 to 4.05) μm.

[b] Variance and standard error of the variance of the individual horse-level random effect term.

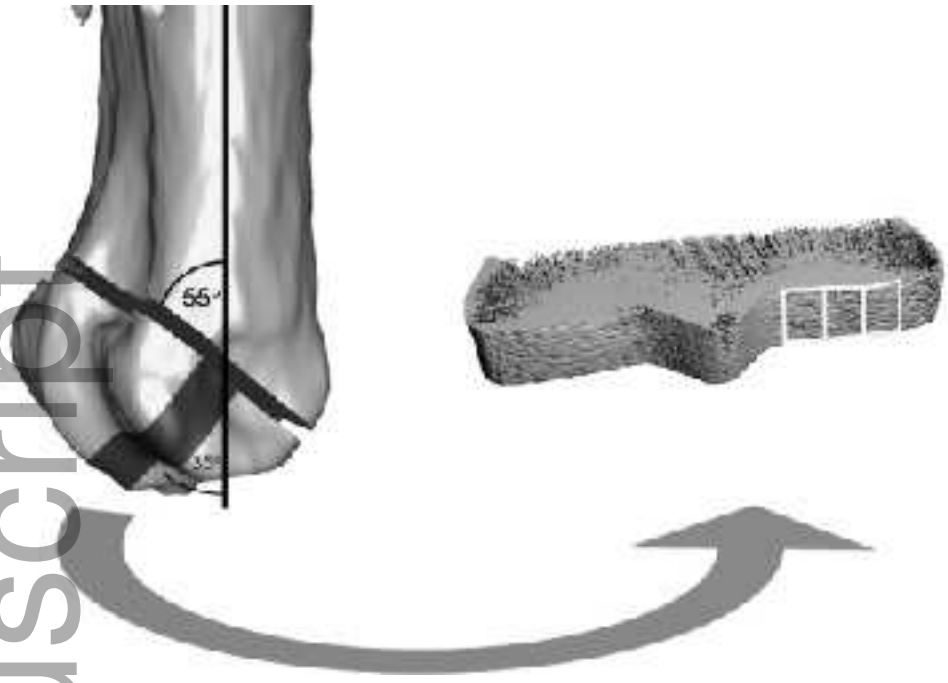

evj_12748_f1.tif

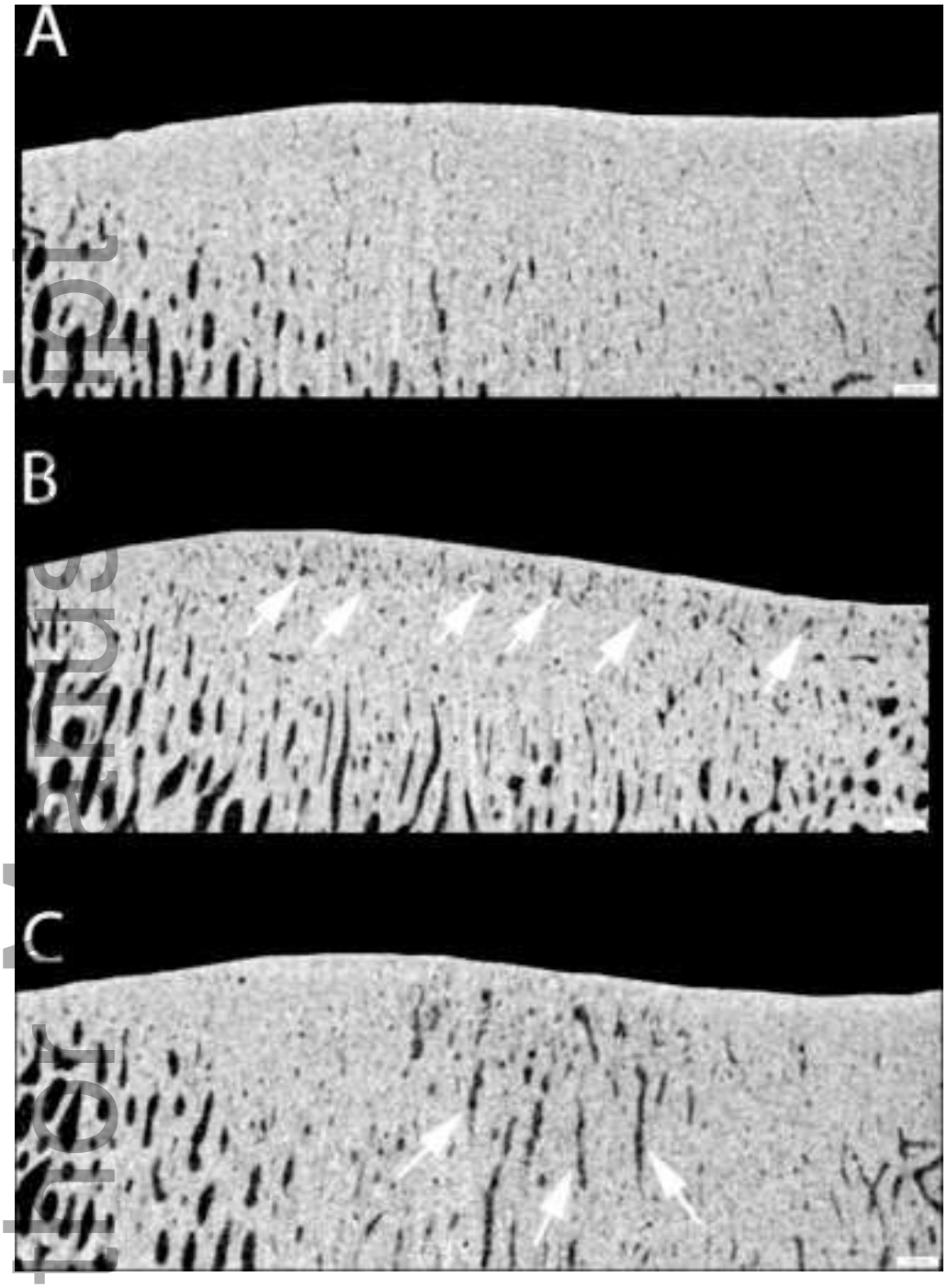

evj_12748_f2.jpg

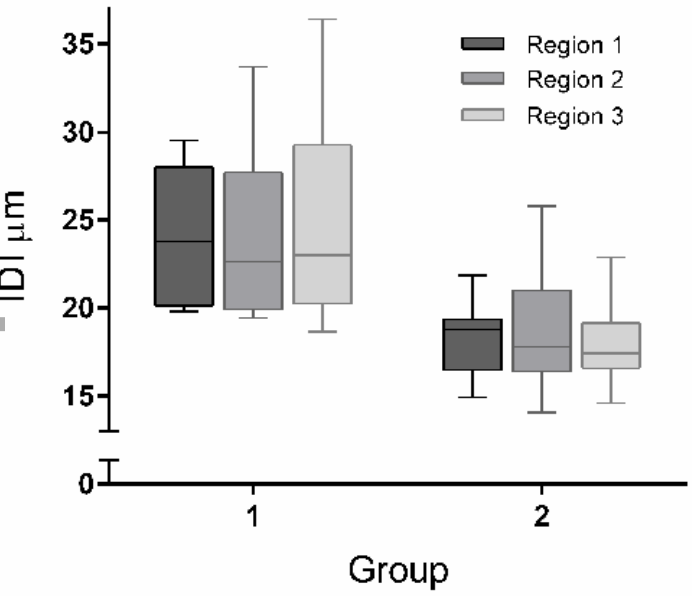

evj_12748_f3.tif

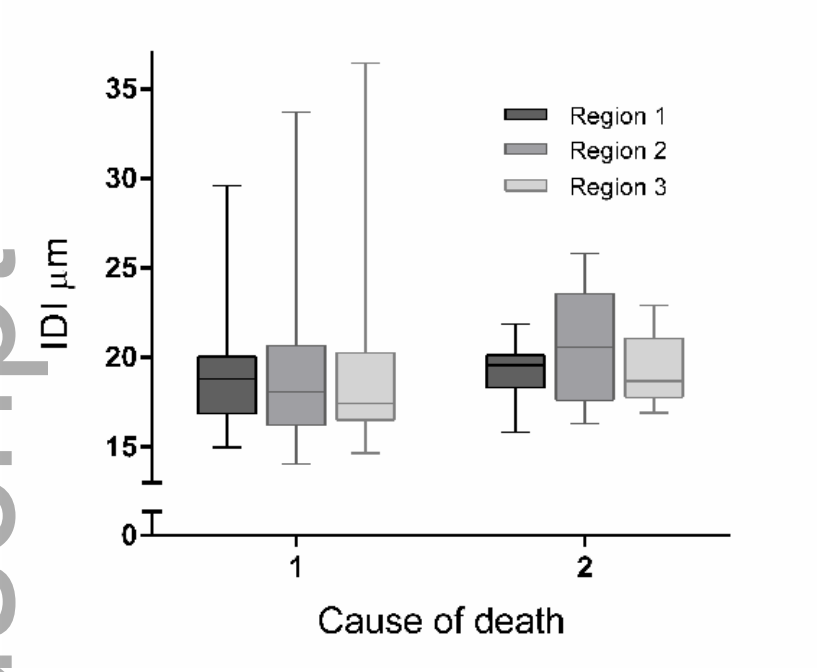

evj_12748_f4.tif